We are IntechOpen, the world's leading publisher of Open Access books Built by scientists, for scientists

4,800
Open access books available

122,000
International authors and editors

135M
Downloads

Our authors are among the

154
Countries delivered to

TOP 1%
most cited scientists

12.2%
Contributors from top 500 universities

CLARIVATE ANALYTICS BOOK CITATION INDEX INDEXED

WEB OF SCIENCE™

Selection of our books indexed in the Book Citation Index in Web of Science™ Core Collection (BKCI)

Interested in publishing with us?
Contact book.department@intechopen.com

Numbers displayed above are based on latest data collected.
For more information visit www.intechopen.com

Chapter 4

EPR Analysis of Antioxidant Compounds

Betül Çalişkan and Ali Cengiz Çalişkan

Additional information is available at the end of the chapter

http://dx.doi.org/10.5772/intechopen.74294

Abstract

A free radical is a molecular species having an unpaired electron and it is a highly reactive entity and unstable. A free radical is a molecule with one or more unpaired electrons in its outer shell. Free radicals can be formed by chemical bond breakage from molecules or by redox reactions. When cells use oxygen, the oxidative stress occurs. The oxidative stress causes free radical formation. Free radicals can also be generated from ionizing radiations, ozone, heavy metal poisoning, cigarette smoking, and chronic alcohol intake. These free radicals are highly reactive and oxidize biomolecules leading to tissue injury and cell death. They also cause toxic effects and diseases. Antioxidants neutralize free radicals resulting from oxidative stress. Antioxidants play an important role in the treatment of diseases. The most suitable method for the analysis of free radicals is the electron paramagnetic resonance (EPR) spectroscopy method. The EPR method detects a paramagnetic center with a single electron. It gives information about the interactions with other nuclei around one electron. It provides information on the structure and environment of radicals.

Keywords: free radical, radiation damage center, antioxidant, electron paramagnetic resonance

1. Introduction

Free radicals are an atom or a molecule that bears an unpaired electron and is extremely reactive, capable of engaging in a rapid change reaction that destabilizes other molecules and generates many more free radicals. In plants and animals, these free radicals are deactivated by antioxidants. These antioxidants act as an inhibitor of the process of oxidation, even at

relatively small concentrations, and thus have diverse physiological roles in the body. The body is constantly exposed to the negative and sometimes lethal effects of oxidants during normal physiological processes. The harmful free radicals such as hydroxyl, peroxyl and the superoxide anion are constantly being produced as a result of metabolic reactions in living systems. On a daily basis, up to 5% of inhaled oxygen may be converted to reactive oxygen species (ROS). These ROS have the ability to bind to cellular structures and have been implicated in a number of pathological processes such as aging, inflammation, reoxygenation of ischemic tissues, atherosclerosis, cancer and even Parkinson's disease in men [1]. Two processes, which produce free radicals in vivo, have been identified and named the Fenton reaction and the Haber-Weiss reaction [2]. Antioxidants play an important role in animal health. Conventional antioxidants have been shown to improve animal performance during conditions characterized by increased tissue oxidant levels such as stress, injury and infections [3].

Free radicals can be classified as reactive oxygen species (ROS), reactive nitrogen species (RNS) and reactive sulfur species (RSS). Even though free radicals are mainly produced through regular metabolic routes, there are also some external factors that promote their production, including smoking, environmental pollutants, radiation and drugs, among others [4]. In healthy organisms, there is a delicate balance between the production and the removal of free radicals, which guarantees that they remain in adequate concentrations. However, when this balance is broken, these reactive species start producing chemical damages to proteins, lipids, DNA, RNA and sugars generating the so-called oxidative stress of body cells [4]. These processes have been associated with several diseases including cardiovascular, liver, neurological and renal disorders, as well as cancer, auto-immune deficiency and degenerative disorders associated with aging, diabetes, obesity, autism, Alzheimer's, Parkinson's and Huntington's diseases [4]. Although humans have developed different endogenous defense mechanisms to protect cells from the excess of free radicals and to avoid the oxidative stress, often these mechanisms are not enough. Therefore, to increase protection from oxidative damage, dietary supplements with antioxidants are recommended as a way to maintain the concentration of free radicals as low as possible [5].

Antioxidants destroy free radicals. Antioxidants neutralize the radical, and thus the radical-antioxidant association maintains itself in a stationary state. For all these situations, antioxidants must be in a structure that will quench the radical. Therefore, unpaired electrons in the structure of antioxidants must be either radical ions or free radicals. So, they must form a paramagnetic center. Paramagnetic structures are analyzed by electron paramagnetic resonance (EPR) spectroscopy. Thus, the EPR analysis of antioxidants is as valuable and important as the investigation of the paramagnetic centers of radicals. There are many studies done for this purpose. Among these studies, especially the works we have done recently are noteworthy.

Potassium hydroquinone monosulfonate (PHM), succinic anhydride and 3-nitroacetophenone compounds are antioxidants. Paramagnetic centers formed by gamma irradiation effect on single crystals of these materials were analyzed by the EPR method [6–8].

2. EPR studies of antioxidant compounds

2.1. Gamma-irradiated potassium hydroquinone monosulfonate single crystal

Free radicals or other odd electrons have often been postulated as intermediates in the decomposition of organic compounds by ionizing radiation. It is still important for formulating mechanisms in radiation chemistry to identify the radicals that are formed. If several organic compounds are irradiated and resulting radicals are identified, one may hope that generalizations can be drawn concerning modes of bond rupture.

The quinone structure is widespread in nature: for example, quinones play an integral role in many biological electron-transfer processes, particularly respiration and photosynthesis [9, 10]. Quinones have long been considered for their fungicide, antibacterial and anticancer properties [11]. The quinone derivatives are especially interesting because they have significant properties due to the ready reversibility of the quinone-semiquinone redox system [12].

The single crystal of PHM was irradiated with gamma rays at room temperature and studied by the EPR technique at 125 K. The spectra were dependent on the orientation of H in the planes, which are perpendicular to each other. The paramagnetic centers formed from PHM are shown in **Figure 1** [6].

The experimental spectrum in **Figure 2** has 1:1:1:2:1 intensity ratios and exhibits the superimposition due to the two PHM anion radicals. Because of the radical A, the spectra exhibit 2-lines with intensity ratios 1:1. Owing to the C6 β-proton, the spectra exhibit a doublet (1:1). Because of the radical B, the spectra exhibit 3-lines with intensity ratios 1:2:1. Owing to the C3 and C4 β-protons, the spectra exhibit a triplet (1:2:1). The spectrum in **Figure 3** has 1:2:2:1 intensity ratios and exhibits the superimposition due to the two PHM anion radicals.

The simulation values of the hyperfine coupling constants of the spectra in **Figures 2** and **3** are given in **Table 1**. The EPR parameters belonging to two semiquinone anion radicals observed in PHM are included in **Tables 2** and **3**.

The EPR measurements have shown the existence of two semiquinone anion radicals. The semiquinone anion radicals were stable. The observed semiquinone anion radicals were obtained from the oxidation of PHM single crystal.

The angular dependences of EPR spectra were obtained for different orientations of the static magnetic field with respect to the crystalline axes. For the radical A and radical B, the spectroscopic splitting factor and the hyperfine coupling constants are anisotropic. For the radical A, the average values of the g-factor and the hyperfine coupling constant were obtained as g_A = 2.01477 and $\left(a_{CH(\beta)}\right)_A$ = 0.326 mT, respectively. For the radical B, the average values of the g-factor and the hyperfine coupling constant were obtained as g_B = 2.01054 and $\left(a_{C_2H_2(\beta)}\right)_B$ = 0.568 mT, respectively.

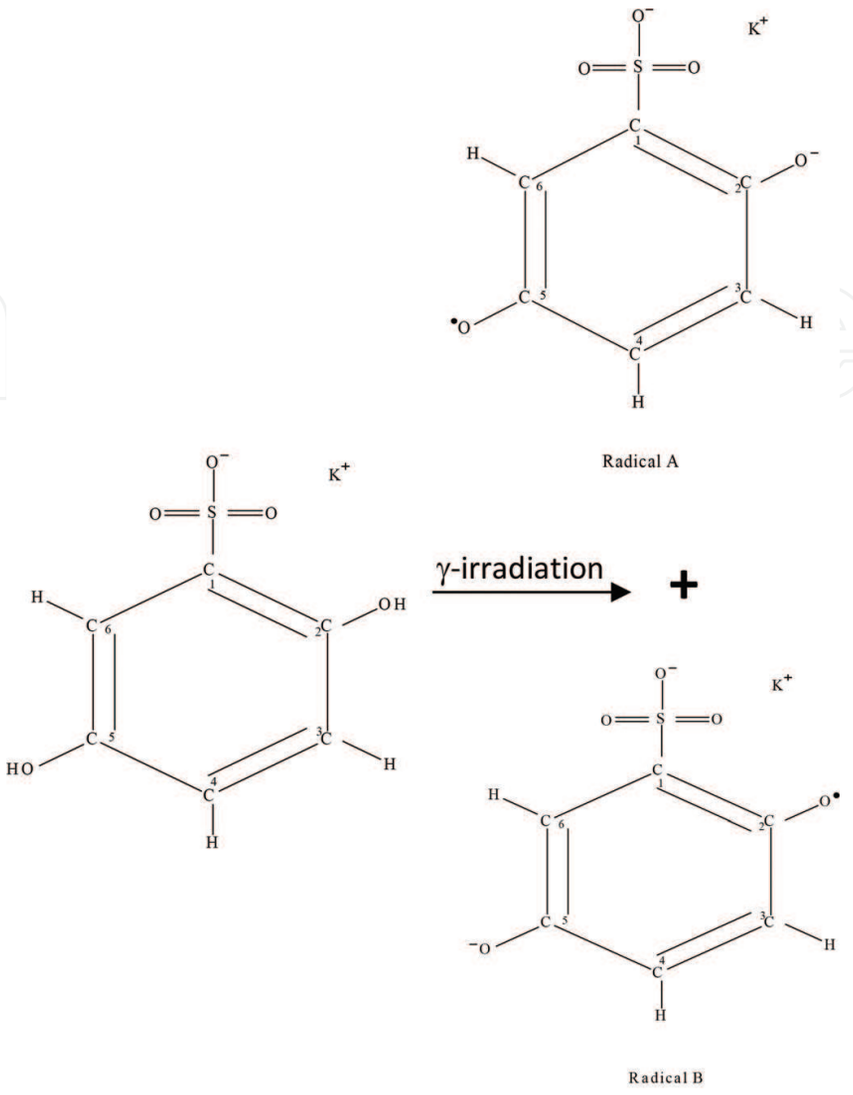

Figure 1. Structure of two semiquinone anion radicals observed in PHM single crystal.

2.2. Gamma-irradiated succinic anhydride single crystal

Succinate:quinone reductase (SQR) of complex II occupies a unique central point in the mitochondrial respiratory system as a major source of electrons driving reactive oxygen species (ROS) production. It is an ideal pharmaceutical target for modulating ROS levels in normal cells to prevent oxidative stress-induced damage or alternatively, increase ROS in cancer cells, inducing cell death [13].

The single crystals of succinic anhydride were irradiated gamma-rays at room temperature and studied by the EPR technique at 125 K [7]. The spectra were dependent on the orientation of H in the planes which are perpendicular to each other The paramagnetic centers formed from succinic anhydride are shown in **Figure 4**.

For only a few angles, the spectra have 1:2:1:1:2:1:2:4:2:2:4:2:1:2:1:1:2:1 intensity ratios. For many angles, the spectra have 1:1:1:1:1:1:1:1:2:2:2:2:2:2:2:2:1:1:1:1:1:1:1:1 intensity ratios. The experimental spectrum in **Figure 5** has 1:2:1:1:2:1:2:4:2:2:4:2:1:2:1:1:2:1 intensity ratios and

http://dx.doi.org/10.5772/intechopen.74294

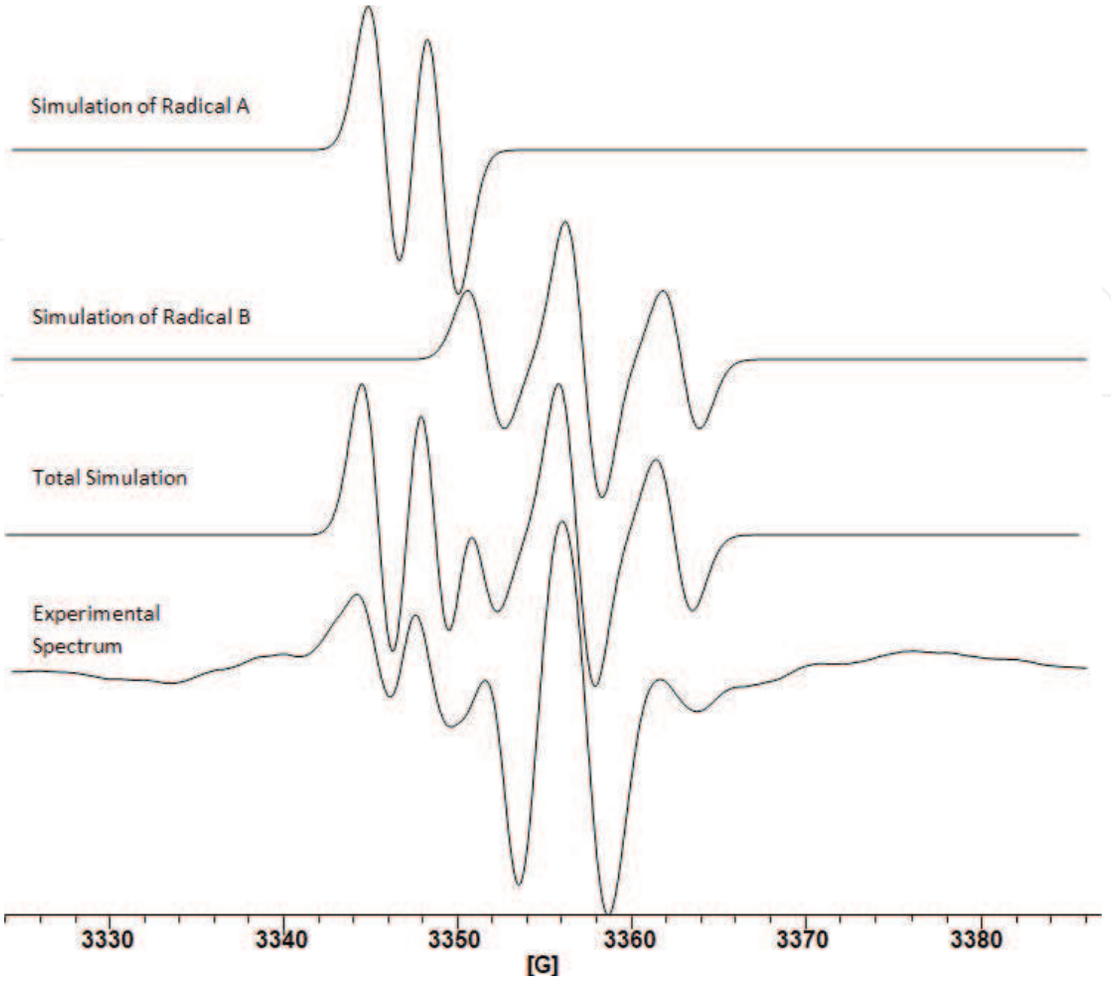

Figure 2. EPR spectrum of gamma-irradiated PHM single crystal at 125 K when the magnetic field is in the ab plane at an angle 0° toward the axis.

exhibits the superimposition due to the two CH_2CH_2 atom groups. Because of the radical A, the spectra exhibit 9-lines with intensity ratios 1:2:1:2:4:2:1:2:1. Owing to the β-protons, the spectra exhibit a triplet (1:2:1). Each of the lines (1:2:1) splits into triplets (1:2:1) due to the two equivalent γ-protons. Because of the radical B, the spectra exhibit 9-lines with intensity ratios 1:2:1:2:4:2:1:2:1. Owing to the β-protons, the spectra exhibit a triplet (1:2:1). Each of the lines (1:2:1) splits into triplets (1:2:1) due to the two equivalent γ-protons. Total 18-lines are observed due to the two anion radicals. The spectrum in **Figure 6** has 1:1:1:1:1:1:1:1:1:2:2:2:2:2:2:2:2:2:1:1:1:1:1:1:1:1:1 intensity ratios and exhibits the superimposition due to the two $(CH_2)_\beta CH_{\gamma 1}H_{\gamma 2}$ atom groups. Because of the radical A, the spectra exhibit 12-lines with intensity ratios 1:1:1:1:2:2:2:2:1:1:1:1. Owing to the β-protons, the spectra exhibit a triplet (1:2:1). Each of the lines (1:2:1) splits into doublets (1:1) due to the γ_1-proton. Each of the lines (1:1:2:2:1:1) splits into doublets (1:1) due to the γ_2-proton. The hyperfine structure splittings in the radical A are the same as that of the radical B. The total 24-lines are observed due to the two anion radicals.

We have obtained the computer simulations of the spectra that give the best agreement with experimental values. The simulations of the EPR spectra have been carried out using the Bruker's WINEPR software.

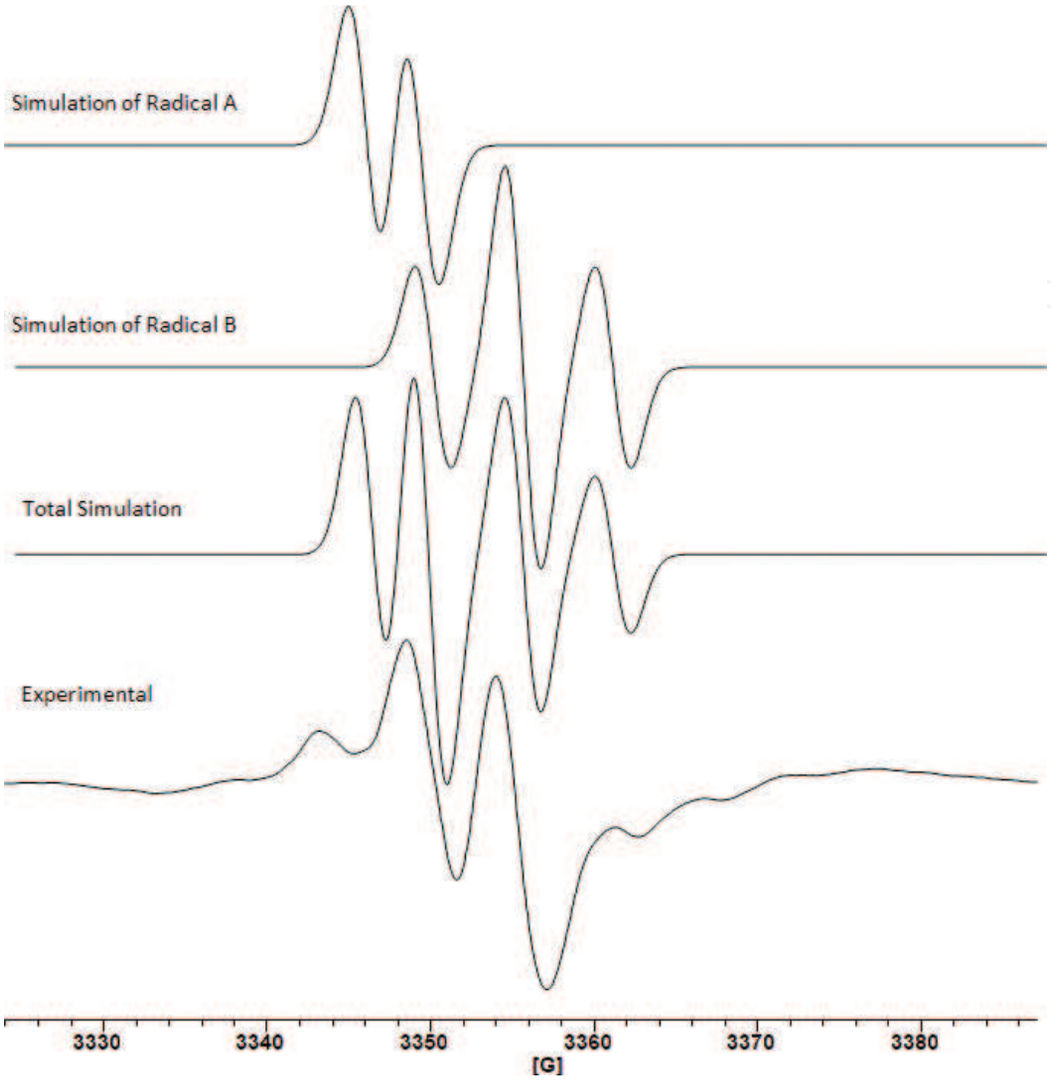

Figure 3. EPR spectrum of gamma-irradiated PHM single crystal at 125 K when the magnetic field is in the ac plane at an angle 70° toward the axis.

	Radical A	**Radical B**
Figure 2	$\left(a_{CH(\beta)}\right)_A$ = 0.328 mT	$\left(a_{CH_{2(\beta)}}\right)_B = \left(a_{H_\beta}\right)_B$ = 0.572 mT
	Center field = 335.5 mT	Center field = 335.5 mT
	ν = 9.38 GHz	ν = 9.408 GHz
	Line width = 0.2 mT	Line width = 0.215 mT
Figure 3	$\left(a_{CH(\beta)}\right)_A$ = 0.327 mT	$\left(a_{CH_{2(\beta)}}\right)_B = \left(a_{H_\beta}\right)_B$ = 0.55 mT
	Center field = 335.5 mT	Center field = 335.5 mT
	ν = 9.38 GHz	ν = 9.401 GHz
	Line width = 0.22 mT	Line width = 0.22 mT

Table 1. EPR parameters of simulated spectra.

	Principal values	Direction cosines		
$\left(A_{CH(\beta)}\right)_A$ (mT)	A_{xx} = 0.347	0.807090	0.452748	−0.378980
	A_{yy} = 0.324	−0.198271	0.812426	0.548318
	A_{zz} = 0.307	0.556143	−0.367402	0.745467
	a_{av} = 0.326			
g_A	g_{xx} = 2.01690	0.745218	0.366680	−0.556952
	g_{yy} = 2.01479	0.353981	0.490298	0.796643
	g_{zz} = 2.01263	0.565109	−0.790667	0.235582
	g_{av} = 2.01477			

Note: The errors are estimated to be ±0.00005 and ±0.005 mT for all the calculated g- and A-values, respectively.

Table 2. The EPR parameters of radical A observed in PHM at 125 K.

	Principal values	Direction cosines		
$\left(A_{C_2H_2(\beta)}\right)_B$	A_{xx} = 0.662	0.618669	0.457813	0.638480
	A_{yy} = 0.56	−0.736026	0.053485	0.674838
	A_{zz} = 0.483	0.274800	−0.887439	0.370051
	a_{av} = 0.568			
g_B	g_{xx} = 2.01119	0.506864	−0.262535	0.821075
	g_{yy} = 2.01056	0.787949	0.527402	−0.317780
	g_{zz} = 2.00986	−0.349608	0.808037	0.474185
	g_{av} = 2.01054			

Note: The errors are estimated to be ±0.00005 and ±0.005 mT for all the calculated g- and A-values, respectively.

Table 3. The EPR parameters of radical B observed in PHM at 125 K.

The simulation values of the hyperfine coupling constants of the spectra in **Figures 5** and **6** are given in **Table 4**. The EPR parameters belonging to two succinic anhydride anion radicals observed in succinic anhydride are included in **Tables 5** and **6**.

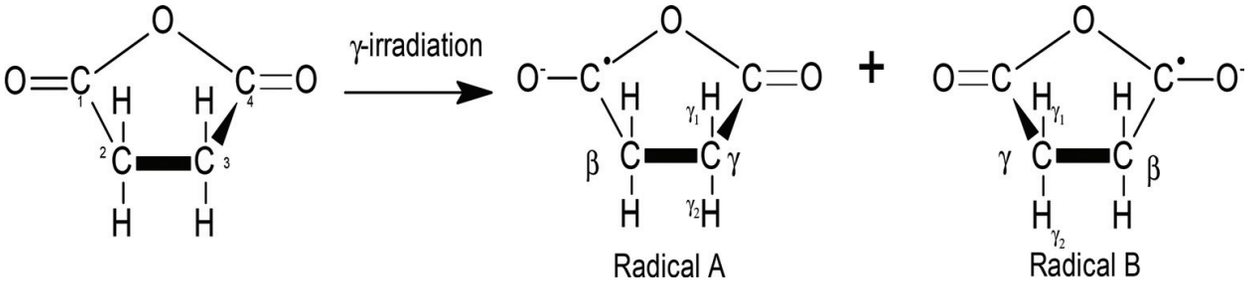

Figure 4. Structure of two succinic anhydride anion radicals observed in succinic anhydride single crystal.

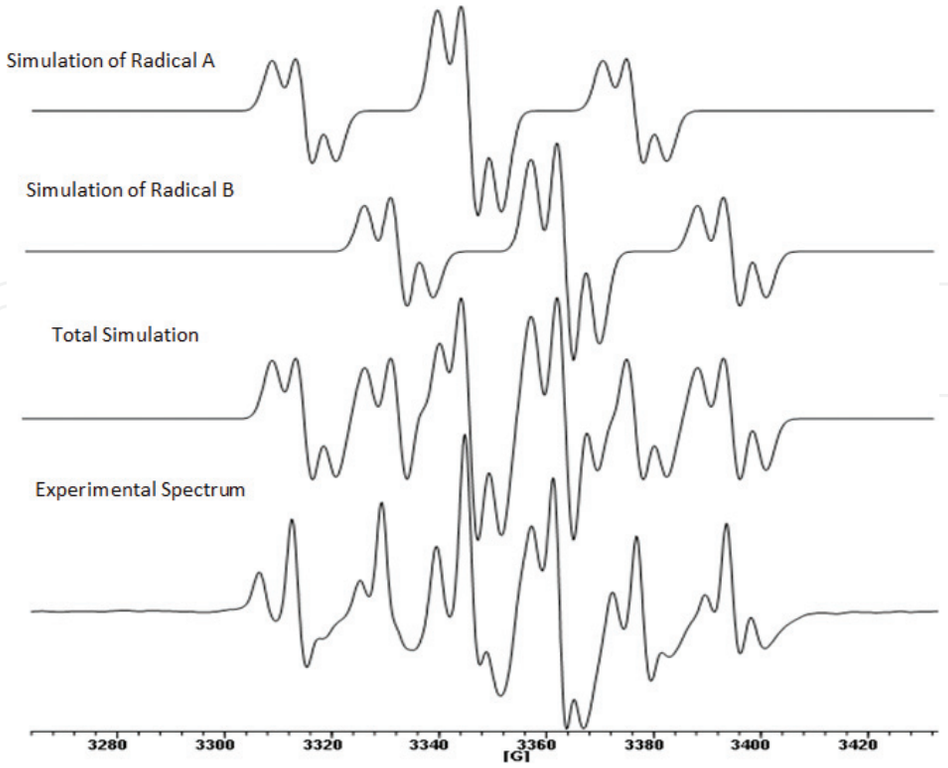

Figure 5. Experimental and simulated EPR spectra of gamma-irradiated succinic anhydride single crystal at 125 K when the magnetic field is in the bc plane at an angle 90° toward the axis.

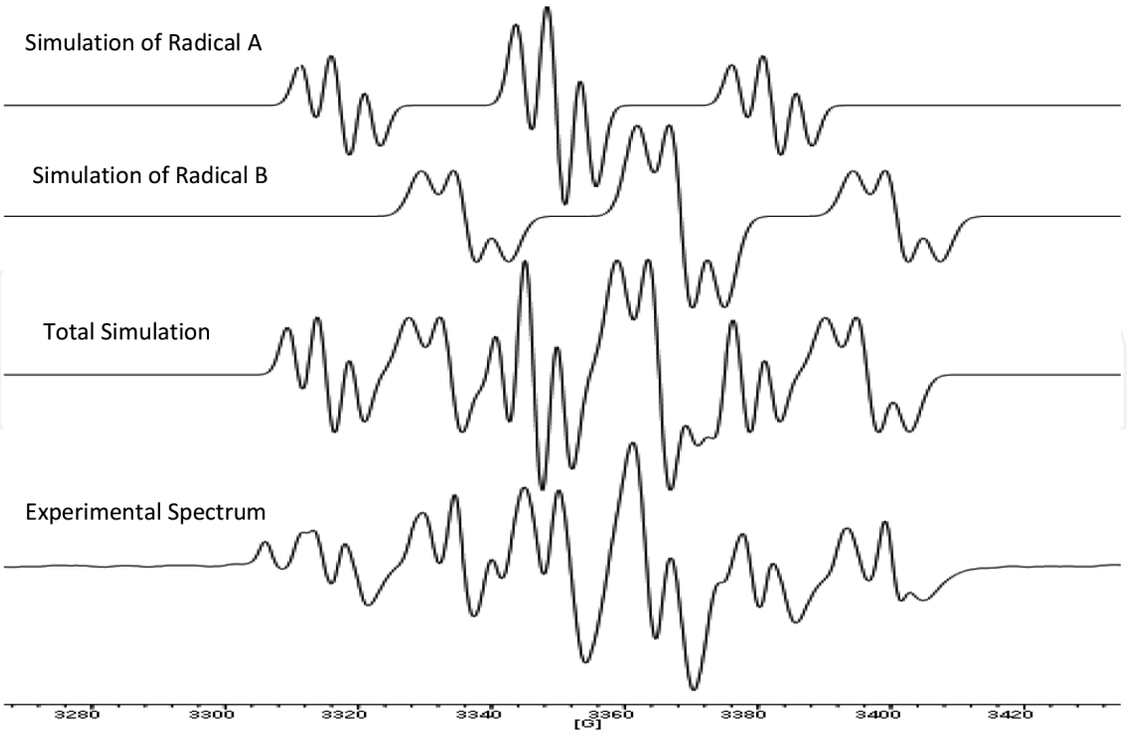

Figure 6. Experimental and simulated EPR spectra of gamma-irradiated succinic anhydride single crystal at 125 K when the magnetic field is in the ac plane at an angle 110° toward the axis.

	Radical A	Radical B
Figure 5	$\left(a_{CH_{2(\beta)}}\right)_A = \left(a_{H_\beta}\right)_A$ = 3.26 mT	$\left(a_{CH_{2(\beta)}}\right)_B = \left(a_{H_\beta}\right)_B$ = 3.281 mT
	$\left(a^{H_{\gamma1}}_{CH_{\gamma1}H_{\gamma2}}\right)_A = \left(a_{H_{\gamma1}}\right)_A$ = 0.47 mT	$\left(a^{H_{\gamma1}}_{CH_{\gamma1}H_{\gamma2}}\right)_B = \left(a_{H_{\gamma1}}\right)_B$ = 0.505 mT
	$\left(a^{H_{\gamma2}}_{CH_{\gamma1}H_{\gamma2}}\right)_A = \left(a_{H_{\gamma2}}\right)_A$ = 0.43 mT	$\left(a^{H_{\gamma2}}_{CH_{\gamma1}H_{\gamma2}}\right)_B = \left(a_{H_{\gamma2}}\right)_B$ = 0.47 mT
	Center field = 335.576 mT	Center field = 335.576 mT
	ν = 9.368 GHz	ν = 9.423 GHz
	Line width = 0.4 mT	Line width = 0.4 mT
Figure 6	$\left(a_{CH_{2(\beta)}}\right)_A = \left(a_{H_\beta}\right)_A$ = 3.245 mT	$\left(a_{CH_{2(\beta)}}\right)_B = \left(a_{H_\beta}\right)_B$ = 3.253 mT
	$\left(a^{H_{\gamma1}}_{CH_{\gamma1}H_{\gamma2}}\right)_A = \left(a_{H_{\gamma1}}\right)_A$ = 0.39 mT	$\left(a^{H_{\gamma1}}_{CH_{\gamma1}H_{\gamma2}}\right)_B = \left(a_{H_{\gamma1}}\right)_B$ = 0.44 mT
	$\left(a^{H_{\gamma2}}_{CH_{\gamma1}H_{\gamma2}}\right)_A = \left(a_{H_{\gamma2}}\right)_A$ = 0.52 mT	$\left(a^{H_{\gamma2}}_{CH_{\gamma1}H_{\gamma2}}\right)_B = \left(a_{H_{\gamma2}}\right)_B$ = 0.5 mT
	Center field = 335.576 mT	Center field = 335.576 mT
	ν = 9.368 GHz	ν = 9.423 GHz
	Line width = 0.3 mT	Line width = 0.42 mT

Table 4. EPR parameters of simulated spectra.

EPR parameters	Principal values	Direction cosines		
$\left(A_{CH_{2(\beta)}}\right)_A = \left(A_{H_\beta}\right)_A$ (mT)	A_{xx} = 3.381	0.194135	0.945231	0.262393
	A_{yy} = 3.285	−0.723568	−0.042637	0.688935
	A_{zz} = 3.227	0.662390	−0.323606	0.675662
	a_{iso} = 3.298			
$\left(A^{H_{\gamma1}}_{CH_{\gamma1}H_{\gamma2}}\right)_A = \left(A_{H_{\gamma1}}\right)_A$ (mT)	A_{xx} = 0.492	0.818223	0.479980	−0.316433
	A_{yy} = 0.44	0.016324	0.530794	0.847344
	A_{zz} = 0. 37	0.574669	−0.698482	0.426473
	a_{iso} = 0.434			
$\left(A^{H_{\gamma2}}_{CH_{\gamma1}H_{\gamma2}}\right)_A = \left(A_{H_{\gamma2}}\right)_A$ (mT)	A_{xx} = 0.62	0.325533	−0.489384	0.809031
	A_{yy} = 0.494	0.775337	0.627894	0.067839
	A_{zz} = 0.414	−0.541185	0.605188	0.583838
	a_{iso} = 0.509			
g_A	g_{xx} = 2.01753	0.998258	0.021593	0.054902
	g_{yy} = 2.01513	−0.054529	0.692912	0.718957
	g_{zz} = 2.01428	−0.022518	−0.720698	0.692883
	g_{iso} = 2.01565			

Table 5. The EPR parameters of radical A observed in succinic anhydride at 125 K.

EPR parameters	Principal values	Direction cosines		
$\left(A_{CH_{2(\beta)}}\right)_B = \left(A_{H_\beta}\right)_B$ (mT)	A_{xx} = 3.36	0.021180	−0.990260	−0.137614
	A_{yy} = 3.283	0.829840	−0.059355	0.554835
	A_{zz} = 3.251	−0.557599	−0.125949	0.820500
	a_{iso} = 3.298			
$\left(A^{H_{\gamma1}}_{CH_{\gamma1}H_{\gamma2}}\right)_B = \left(A_{H_{\gamma1}}\right)_B$ (mT)	A_{xx} = 0.586	0.066077	0.942855	0.326586
	A_{yy} = 0.485	−0.896800	−0.087383	0.433722
	A_{zz} = 0.379	0.437475	−0.321541	0.839778
	a_{iso} = 0.483			
$\left(A^{H_{\gamma2}}_{CH_{\gamma1}H_{\gamma2}}\right)_B = \left(A_{H_{\gamma2}}\right)_B$ (mT)	A_{xx} = 0.612	0.759274	−0.102410	0.642663
	A_{yy} = 0.464	−0.632874	0.113810	0.765844
	A_{zz} = 0.288	−0.151571	−0.988210	0.021600
	a_{iso} = 0.455			
g_B	g_{xx} = 2.00660	0.977193	0.210889	−0.024888
	g_{yy} = 2.00410	−0.096452	0.545205	0.832736
	g_{zz} = 2.00300	0.189184	−0.811343	0.553111
	g_{iso} = 2.00457			

Table 6. The EPR parameters of the radical B observed in succinic anhydride at 125 K.

The radical formation mechanism in the present work is the same as that of potassium hydroquinone monosulfonate [6]. The angular dependences of EPR spectra were obtained for different orientations of the static magnetic field with respect to the crystalline axes. For the radical A and radical B, the spectroscopic splitting factor and the hyperfine coupling constants of the H_β, $H_{\gamma1}$ and $H_{\gamma2}$ protons are anisotropic. For the radical A, the average values of the g-factor and the hyperfine coupling constants were obtained as g_A = 2.01565, $\left(a_{H_\beta}\right)_A$ = 3.298 mT, $\left(a_{H_{\gamma1}}\right)_A$ = 0.434 mT, $\left(a_{H_{\gamma2}}\right)_A$ = 0.509 mT, respectively. For the radical B, the average values of the g-factor and the hyperfine coupling constants were obtained as g_B = 2.00457 and $\left(a_{H_\beta}\right)_B$ = 3.298 mT, $\left(a_{H_{\gamma1}}\right)_B$ = 0.483 mT, $\left(a_{H_{\gamma2}}\right)_B$ = 0.455 mT, respectively.

2.3. Gamma-irradiated 3-nitroacetophenone single crystal

Nitroaromatic compounds have widespread actual or potential use in medicine and cancer therapy [14]. Nitroaromatic compounds have been extensively studied and reviewed mainly because of their interesting biological activities as well as their extended use in the chemical industry [15].

The radical in 3NAP identified as 3-nitroacetophenone anion radical is shown in **Figure 7**. The spectra were found to be temperature dependent. When we examined the EPR spectra at a

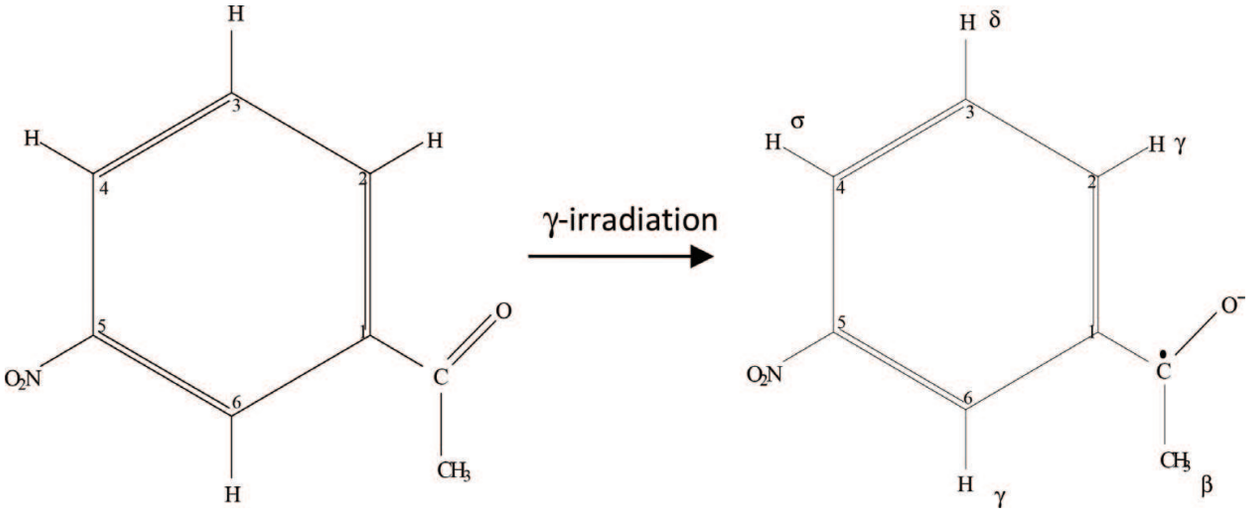

Figure 7. Structure of the 3NAP anion radical observed in 3NAP.

temperature range of 120–360 K, we decided that the radiation damage center in the sample was due to the break of the pi bond in the carbon-oxygen double bond. It was seen that the unpaired electron interacted with all the protons in the molecular structure [8].

In the EPR spectra, especially the impact of the methyl protons was felt. The hyperfine coupling constants of the methyl protons were measured at 300 K. The angular variations of EPR parameters of the 3NAP only at 300 K could be investigated. The spectra were clear only in a few angles, at 120 K. Therefore, only the simulations of these spectra were made, at 120 K. In addition, the simulation was also made for a single angle, at 300 K.

The EPR spectra of irradiated 3-nitroacetophenone single crystals consist of four hyperfine structure lines with a 1:3:3:1 intensity ratio, which is caused by the interaction of the unpaired electron with the three equivalent protons of the methyl group, at most orientations of the crystal in the magnetic field, at 300 K. The H(2) and the H(6) protons are also considered approximately equivalent.

In **Figures 8–11**, the experimental spectra of the gamma-irradiated 3NAP single crystals and their simulation spectra were compared.

The simulation values of the hyperfine coupling constants of the spectra in **Figures 8–11** are given in **Table 7**. The EPR parameters of the 3-nitroacetophenone anion radical are given in **Table 8**.

In the EPR spectra, especially the impact of the methyl protons was felt. Only the hyperfine coupling constants of the methyl protons could be experimentally measured at 300 K. The EPR spectra of irradiated 3-nitroacetophenone single crystals consist of four hyperfine structure lines with a 1:3:3:1 intensity ratio, which is caused by interaction of the unpaired electron with the three equivalent protons of the methyl group, at most orientations of the crystal in the magnetic field, at 300 K. The H(2) and the H(6) protons are also considered approximately equivalent. The hyperfine coupling for the CH_3 group is anisotropic and their average values being a_{CH_3} = 1.402 mT.

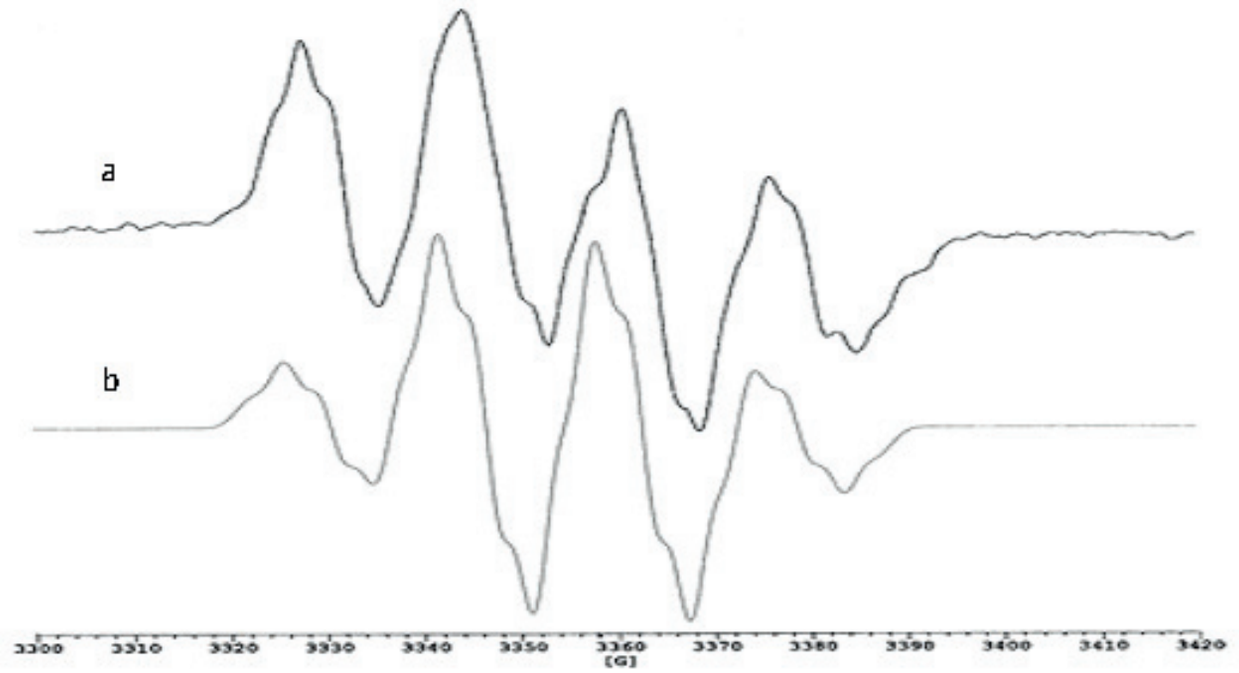

Figure 8. EPR spectra of ^{60}Co-γ irradiated 3NAP single crystal at 300 K when (a) the magnetic field is in the a*b-plane and is away 20° from the a*-axis and (b) simulation of the spectrum; line width is 0.34 mT.

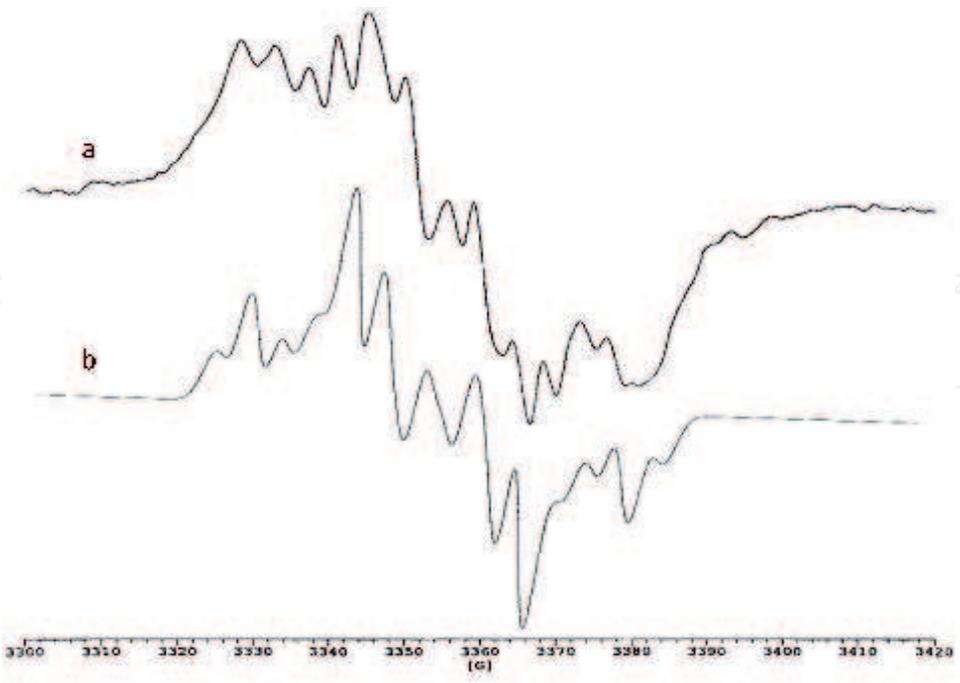

Figure 9. EPR spectra of ^{60}Co-γ irradiated 3NAP single crystal at 120 K when (a) the magnetic field is in the a*c-plane and is away 140° from the a*-axis and (b) simulation of the spectrum; line width is 0.38 mT.

http://dx.doi.org/10.5772/intechopen.74294

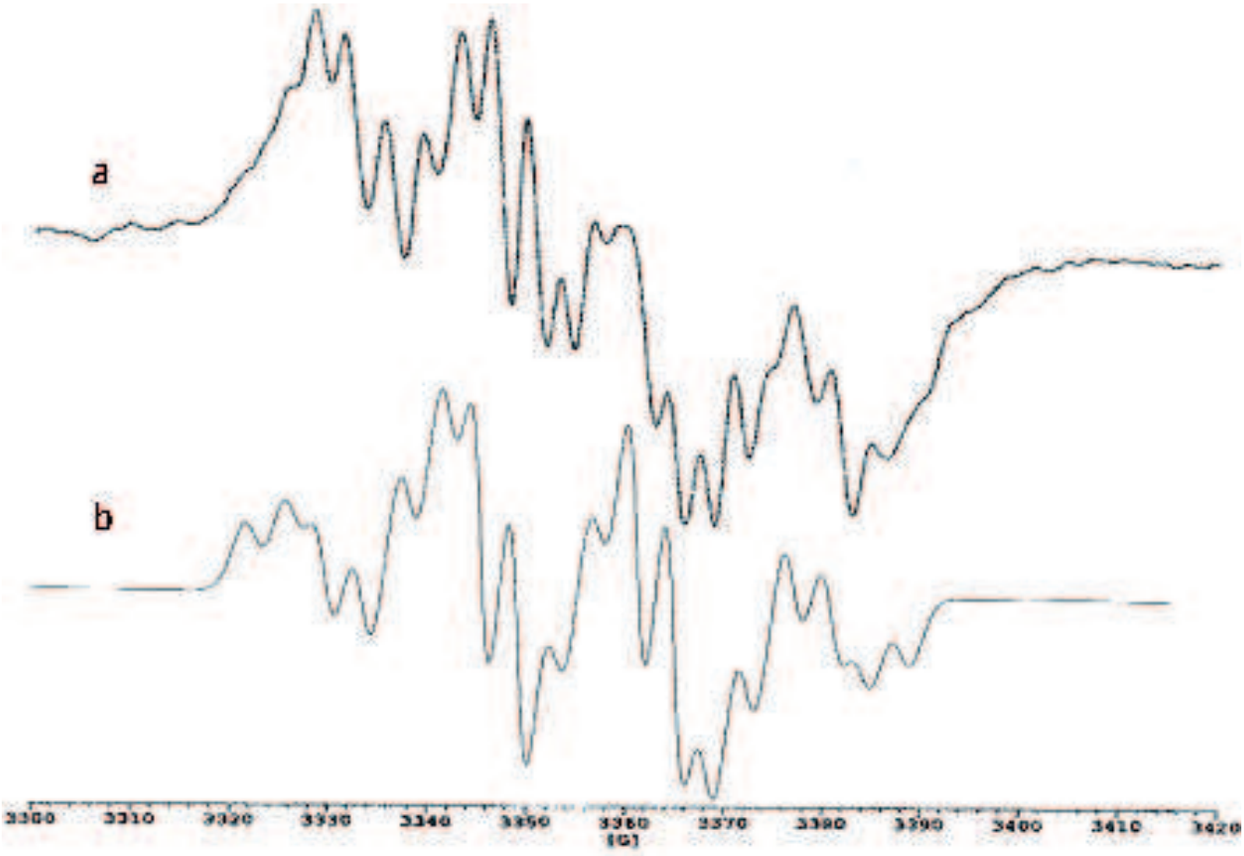

Figure 10. EPR spectra of ^{60}Co-γ irradiated 3NAP single crystal at 120 K when (a) the magnetic field is in the a*c-plane and is away 150° from the a*-axis and (b) simulation of the spectrum; line width is 0.32 mT.

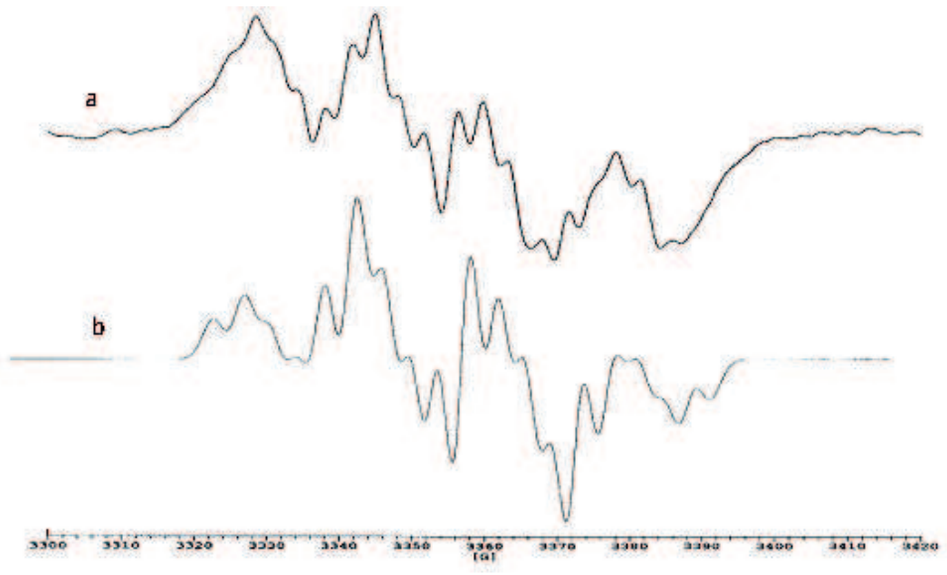

Figure 11. EPR spectra of ^{60}Co-γ irradiated 3NAP single crystal at 120 K when (a) the magnetic field is in the a*c-plane and is away 165° from the a*-axis and (b) simulation of the spectrum; line width is 0.34 mT.

	Figure 8	Figure 9	Figure 10	Figure 11
$a_{CH_3(\beta)}$ mT	1.55	1.36	1.68	1.585
$a_{H(2)} \cong a_{H(6)} = a_{C_2H_2(\gamma')}$ mT	0.38	0.43	0.45	0.46
$a_{H(3)} = a_{H(\delta)}$ mT	0.35	0.68	0.71	0.68
$a_{H(4)} = a_{H(\sigma)}$ mT	0.25	0.39	0.265	0.29

Table 7. Coupling constants values of simulated spectra.

	Principal values	Direction cosines		
$a_{CH_3(\beta)}$ (mT)	A_{xx} = 1.743	0.673208	−0.717129	−0.180325
	A_{yy} = 1.447	0.572490	0.659816	−0.486721
	A_{zz} = 1.015	0.468023	0.224430	0.854743
	a_{iso} = 1.402			
	ρ = 0.52			
g	g_{xx} = 2.006443	0.732137	0.415100	−0.540063
	g_{yy} = 2.006110	0.299886	0.515457	0.802728
	g_{zz} = 2.004067	0.611591	−0.749664	0.252902
	g_{iso} = 2.005540			

Table 8. The EPR parameters of the 3-nitroacetophenone anion radical observed in 3-nitroacetophenone at 300 K.

The simulations of the EPR spectra were carried out using the Win-EPR software.

3. Conclusion

There are many factors that trigger the formation of free radicals. One of these is the radiation effect. The various compounds that undergo radiation effects have the radiation damage centers as a result of breaking bonds in their structures. The radiation damage center is a paramagnetic center, and the detection and motion of these centers are investigated in detail by EPR spectroscopy.

Antioxidants also show paramagnetic structure under radiation effect. EPR analysis of antioxidants is crucial to remove the effect of free radicals that cause many diseases. Potassium hydroquinone monosulfonate (PHM), succinic anhydride and 3-nitroacetophenone compounds show antioxidant properties. When EPR analyses of these materials were made, it was seen that their radical mechanisms were similar to each other. The anion radicals were observed in all three compounds. When the resonance structure and the formation mechanisms are carefully examined, it is seen that the oxygen atom takes an electron and forms a stable anion structure.

Author details

Betül Çalişkan[1]* and Ali Cengiz Çalişkan[2]

*Address all correspondence to: bcaliska@gmail.com

1 Department of Physics, Faculty of Arts and Science, Pamukkale University, Denizli, Turkey

2 Department of Chemistry, Faculty of Science, Gazi University, Ankara, Turkey

References

[1] Setiadi DH, Chass GA, Torday LL, Varro A, Papp JG. Vitamin E models. Can the antioxidant and pro-oxidant dichotomy of α-tocopherol be related to ionic ring closing and radical ring opening redox reactions? Journal of Molecular Structure. 2003;**620**(2-3):93-106

[2] Halliwell B, Gutteridge JMC. Free radicals in Biology and Medicines. 4th ed. Oxford: Oxford University Press; 1985. pp. 120-123

[3] Nickel W. The mystery of non-classical protein secretion: A current view on cargo proteins and potential export routes. European Journal of Biochemistry. 2003;**270**(10):2109-2119

[4] Pham-Huy LA, He H, Pham-Huy C. Free radicals, antioxidants in disease and health. International Journal of Biomedical Science. 2008;**4**(2):89-96

[5] Pietta PG. Flavonoids as antioxidants. Journal of Natural Products. 2000;**63**(7):1035-1042

[6] Caliskan B, Caliskan AC, Er E. Electron paramagnetic resonance study of gammair-radiated potassium hydroquinone monosulfonate single crystal. Radiation Effects and Defects in Solids. 2016;**171**(5-6):440-450. DOI: 10.1080/10420150.2016.1203924

[7] Caliskan B, Caliskan AC, Er E. Electron paramagnetic resonance study of radiation-induced paramagnetic centers in succinic anhydride single crystal. Journal of Molecular Structure. 2017;**1144**:421-431. DOI: 10.1016/j.molstruc.2017.05.039

[8] Caliskan B, Caliskan AC. EPR study of radiation damage in gamma irradiated 3-nitroacetophenone single crystal. Radiation Effects and Defects in Solids. 2017;**172**(5-6):398-410. DOI: 10.1080/10420150.2017.1320800

[9] Thomson RH. Naturally Occurring Quinones. 2nd ed. New York: Academic Press; 1971

[10] Morton RA. Biochemistry of Quinones. New York: Academic Press; 1965

[11] O'Brien PJ. Molecular mechanisms of quinone cytotoxicity. Chemico-Biological Interactions. 1991;**80**(1):1-41

[12] Hashimoto K, Togo H, Morihashi K, Yokoyama Y, Kikuchi O. Conformational change of benzoquinone crown ether radical anions induced by complexation with alkali metal

cation: An ESR study. Bulletin of the Chemical Society of Japan. 1991;**64**(11):3245-3250. DOI: 10.1246/bcsj.64.3245

[13] Ralph SJ, Moreno-Sánchez R, Neuzil J, Rodríguez-Enríquez S. Inhibitors of succinate: Quinone reductase/Complex II regulate production of mitochondrial reactive oxygen species and protect normal cells from ischemic damage but induce specific cancer cell death. Pharmaceutical Research. 2011;**28**(12):3274-3274. DOI: 10.1007/s11095-011-0566-7

[14] Wardman P. Some reactions and properties of nitro radical-anions important in biology and medicine. Environ. Health Perspect. 1985;**64**:309-320

[15] Dincer S. The preferential reduction of 4,6 (5,7)-dinitro and 5,6-dinitrobenzimidazoles. Dyes Pigments. 2002;**53**:263-266